JOURNAL OF PROPULSION AND POWER
Vol. 11, No. 6, November–December 1995

Supersonic Flow Mixing and Combustion Using Ramp Nozzle

Ken H. Yu,* Klaus C. Schadow,† Karl J. Kraeutle,‡ and Effie J. Gutmark*
U.S. Naval Air Warfare Center, China Lake, California 93555-6001

A special supersonic nozzle that features five swept ramps on its expansion side, called the RAMP nozzle, was used to enhance Mach 2 jet mixing with the surrounding air either at rest or flowing at Mach 1.3. The total pressure profiles of the supersonic jets were measured at several streamwise stations and the initial shear-layer growth rates were deduced from the measurements. The results showed that the special growth rate was significantly increased with the RAMP nozzle in comparison with axisymmetric supersonic jets discharging from reference circular nozzles. The increase was 44% at the convective Mach number of 0.23 and 110% at 0.86. Also, the supersonic jets were visualized using a planar Mie-scattering technique. Instantaneous images of the RAMP-expanded-jet showed large-scale well-organized structures that resembled axial vortices in the shear layers. The appearance of these structures was linked to the increase in the initial shear-layer growth rate. Lastly, for an afterburning fuel-rich supersonic jet, the RAMP nozzle changed the afterburning characteristics significantly. This suggests that the supersonic mixing is affected.

Introduction

RECENTLY there has been renewed interest in supersonic combustion research, motivated by the supersonic combustion ramjet (SCRAMJET) development program. In SCRAMJETs, heat is to be added to the incoming supersonic airstream by means of either fuel-rich products (supersonic gas-generator ramjets) or direct fuel injection, which results in simultaneous mixing and burning. While supersonic shear flows have an inherently low mixing rate requiring a long distance for complete mixing, a drag consideration at high speed makes a short combuster length desirable. Thus, finding some means to achieve fast mixing remains a challenging problem.

The fact that supersonic shear flows spread at a slower rate than incompressible shear layers is due to the compressibility effect. This has been well established by many previous experiments, both in planar shear layers[1–3] and in coaxial shear layers.[4] The level of compressibility in a shear layer is given by the convective Mach numbers, which are relative freestream Mach numbers in a frame of reference moving at the large-scale structure velocity. For instance, assuming large-scale structures exist in the shear layer, if they convect at velocity U_C, then $M_{C1} = (U_1 - U_C)/a_1$ and $M_{C2} = (U_C - U_2)/a_2$, where U_1 and U_2 are the freestream velocities in a stationary frame. If there is no shock in the flow, the reservoir pressures of the two freestreams in the convective frame of reference can be matched, allowing the calculation of U_C. More specifically,

$$p_1\left(1+\frac{\gamma_1-1}{2}M_{C1}\right)^{\gamma_1/(\gamma_1-1)} = p_2\left(1+\frac{\gamma_2-1}{2}M_{C2}\right)^{\gamma_2/(\gamma_2-1)}$$

where p_1 and p_2 are the static pressures, a_1 and a_2 are the speeds of sound, and γ_1 and γ_2 are the ratios of specific heats in respective streams.[1,3,5,6] When $p_1 = p_2$ and $\gamma_1 = \gamma_2$, M_{C1} and M_{C2} become equal so that

$$U_C = \frac{a_1 a_2(M_1 + M_2)}{a_1 + a_2}$$

where M_1 and M_2 are actual Mach numbers of the flow, i.e., U_1/a_1 and U_2/a_2.

Previous studies using various nozzle shapes and attachments have shown that mixing enhancement is possible via axial vortices or three dimensionality in the flow. For subsonic flow, Ho and Gutmark[7] used an elliptic nozzle having the same cross-sectional area as a round nozzle to enhance the near-field entrainment. Schadow et al.[8] studied a triangular jet and showed that small-scale eddies were dominant near the vertices. Bradbury and Khadem[9] inserted small rectangular tabs into a jet flow producing significant distortions in the jet development. Longmire et al.[10] used crown-shaped nozzle attachments to vary the axial position of the nozzle exit around the circumference, thereby observing local increases in entrainment. In experiments involving supersonic flow, Gutmark et al.[4] showed that rectangular jets enhanced mixing compared to circular jets. Samimy et al.[11] reported an increased entrainment by attaching tabs or vortex generators at the nozzle exit. Using wall-mounted ramp injectors, Northam et al.[12] showed enhanced mixing for the swept ramp configuration. In hypersonic applications, Marble et al.[13] suggested axial vorticity production by the baroclinic source term as a possible mechanism to achieve fast mixing. Their fuel injection scheme used ramps to create oblique shocks that crossed cylindrical fuel jets, thereby creating the baroclinic torque in the streamwise direction. The work was further carried out by Waitz et al.,[14] both experimentally and numerically.

In the present article, we examine the effect of nozzle geometry on supersonic flow mixing and its implication on supersonic reaching jets. Two converging–diverging c/d nozzles that were designed to incorporate various mixing enhancement mechanisms were tested and compared with the reference case using a round c/d nozzle. Assuming the amount of mixing was related to the shear-layer thickness (i.e., if we did not distinguish between large-scale "stirring" and molecular-level "mixing" processes), the spatial growth rate of the shear layer $\delta' = d\delta/dx$ can be used to quantitatively compare the turbulent compressible mixing between nonreacting supersonic flows. Furthermore, the effects on reacting flows

Received March 26, 1994; revision received Feb. 15, 1995; accepted for publication Feb. 23, 1995.

*Research Scientist, Research and Technology Division. Member AIAA.
†Supervisory General Engineer, Research and Technology Division. Member AIAA.
‡Research Chemist, Retired.

and the physical mechanisms associated with the observed changes were qualitatively studied.

Experimental Setup and Visualization

Experimental Setup

The experiments were performed using a coaxial supersonic jet stand shown in Fig. 1. The stand consisted of two supersonic flow nozzles aligned in a coaxial manner. The outer nozzle was a contoured *c/d* nozzle designed for Mach 1.3 airflow at the exit. The inner nozzle was attached at the end of a long straight section inside the outer nozzle and was easily replaced with other nozzles having different expansion designs. All the inner nozzles that were used in the experiments were designed for Mach 2.0 airflow at the exit.

Table 1 shows the flow conditions for three different test cases. The first two were nonreacting tests, as air was used for both jets. In the last case, high-temperature products of hydrogen–oxygen reaction, diluted with nitrogen for controlling the exit temperature, were used for the inner jet. The gas discharging from the nozzle exit contained unburned hydrogen from a fuel-rich primary reaction with the equivalence ratio of 2.0. A small amount of carbon particles was added for visualization purposes. An afterburning reaction was observed in the downstream of the jet as the high-temperature fuel-rich gas reacted with the ambient air. Typically, the afterburning reaction initiated about five nozzle-exit diameters downstream of the nozzle.

For the inner jet, the ratio between the stagnation pressure and the static pressure was maintained to produce Mach 2.0 at the jet exit. Consequently, the jets in case I were always fully expanded, while in other cases a slight mismatching of the exit pressure sometimes resulted. In case II, depending on the exterior design of the inner-nozzle base that affected the area ratio of the outer nozzle, a slight-to-moderate overexpansion of the outer jet was observed. In case III, the specific heat ratio of the exit gas was 1.28, making the design Mach number for the inner nozzle 1.94. As a result, the jets in case III were slightly underexpanded.

Figure 2 shows three different inner nozzles. The dimensions for the three nozzles were identical on the flow-converging end up to and including the nozzle throat, but on the expansion side only the cross-sectional area ratio was kept constant at each corresponding streamwise location. One of the nozzles was a conical-expansion circular nozzle with the exit diameter of 25 mm (called the "CIRC" nozzle) and was used as the reference for the other two. The other two nozzles were characterized by notches and ramps on the expansion-side interior wall. Figure 2b shows the nozzle with five small notches for vortex generation ("NTCH" nozzle), and Fig. 2c shows the nozzle with five ramps ("RAMP" nozzle) similar to the swept-ramp configuration in planar flow studied by other investigators.[14–16] The exteriors of the nozzles were round and tapered with a simple boat-tail angle of either 2 or 6 deg.

Table 1 Flow conditions

Case	M_1	a_1, m/s	M_2	a_2, m/s	M_{C1}
I	2.0	250	0	340	0.86
II	2.0	250	1.3	290	0.23
III	2.0	980	0	340	1.5

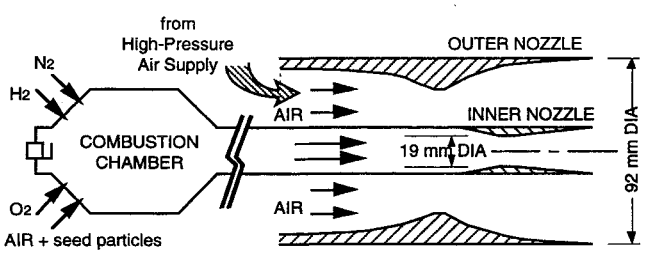

Fig. 1 Coaxial supersonic jet stand (not in scale).

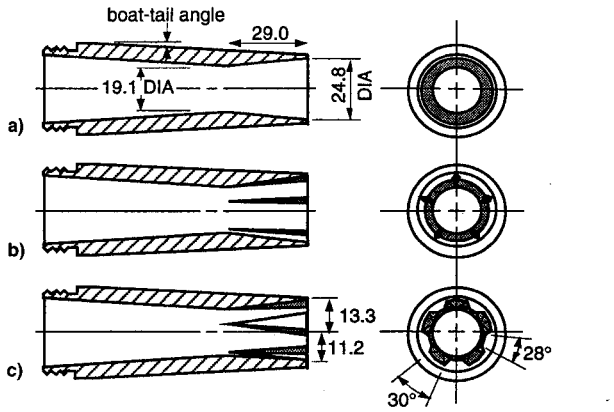

Fig. 2 Converging–diverging nozzles for the inner jet (dimensions in mm). The pitot survey was taken along the vertical axis shown on the frontal view: a) circular reference nozzle CIRC, b) NTCH nozzle, and c) RAMP nozzle.

Mie Scattering Flow Visualization

A planar Mie scattering flow visualization was performed to visualize the supersonic jets and the shear layers. A copper vapor laser (20-ns pulse, 8-kHz repetition) was used as the light source. The laser beam was focused into a thin sheet that passed through the jets along the streamwise axis illuminating a distance of about 150 mm from the exit.

For cases I and II, the inner jet was seeded with condensed ethanol droplets. The total mass flux for ethanol was about 0.5% of the inner jet airflow rate. First, the upstream flow was nearly saturated with ethanol vapor. Then the vapor-laden flow was expanded through a supersonic nozzle lowering the flow temperature and the ethanol saturation pressure. The supersaturated amount of ethanol condensed quickly into a fine mist making the flow visible. The technique is described in Ref. 17. The final droplet size was estimated by other investigators[17,18] to be about 0.1–0.2 μm in diameter. The outer flow was unseeded making the seeding technique a "passive scalar transport" type. Scattered laser light from the droplets was imaged at a right angle using a charge-coupled device camera.

Results and Discussion

Total Pressure Profiles

Total pressure measurements were made with a Kulite XCQ-080 pressure transducer that was traversed across the jets passing through the center axis. The surveys were performed across the vertical axis shown in Fig. 2 at several streamwise stations. The total and rms pressure profiles for the case I condition are shown in Figs. 3 and 4. When a reference nozzle (CIRC) was used, the jet core was maintained up to 10 exit diameters downstream from the exit. Little or no effect on jet development was observed with the NTCH nozzle, and thus, only the RAMP nozzle data were compared in subsequent tests. When the RAMP nozzle was used, high intensity fluctuations from the initial shear layer dispersed more quickly breaking up the jet core at about six exit diameters downstream.

For the case II condition, the exterior geometry of the inner nozzle affected the outer jet profiles. Five different configurations, shown in Fig. 5, were used to study the effect of nozzle exterior geometry on shear-layer characteristics. By using a flow straightener, the level of initial turbulent fluctuations for the outer jet was reduced from 4.0% of the free-stream mean in configuration 1 to 3.0% in configuration 2. In configuration 3, the boat-tail angle was changed from 6 to

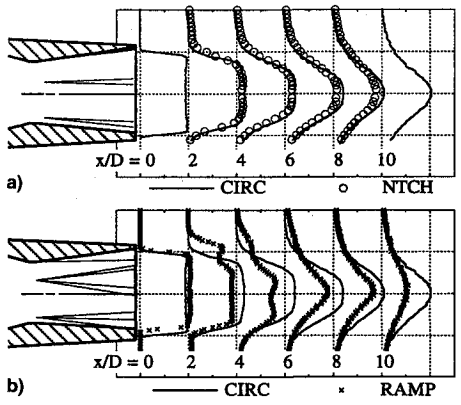

Fig. 3 Total pressure profile for case I flows at various axial locations: a) with NTCH nozzle and b) with RAMP nozzle.

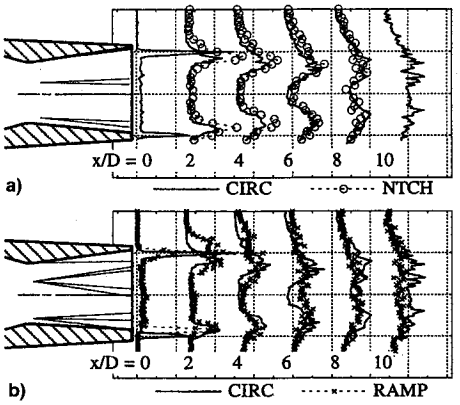

Fig. 4 RMS fluctuations of the total pressures shown in Fig. 3: a) NTCH nozzle and b) RAMP nozzle.

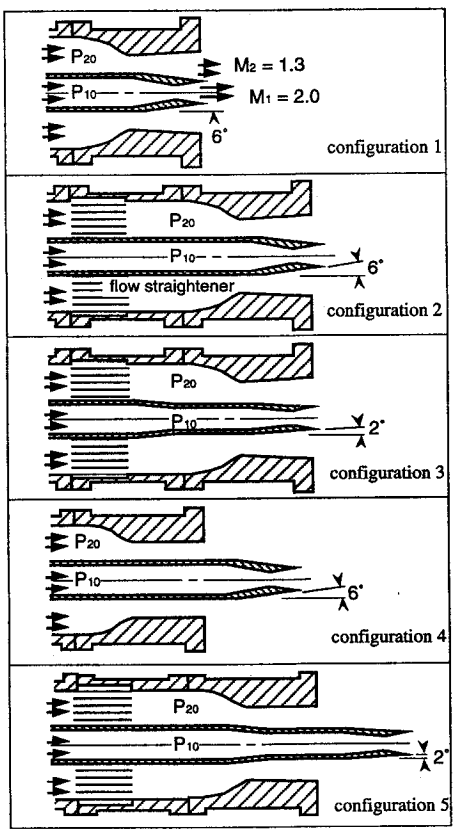

Fig. 5 Five different configurations for coaxial jet experiments.

2 deg. Because the inner nozzle boat-tail section was placed inside the outer nozzle expansion zone, it affected the expansion rate for the outer flow. In configurations 4 and 5, the boat-tail section was moved downstream outside of the expansion zone.

Streamwise flow developments for cases I and II are compared in Fig. 6 using a CIRC nozzle. When the outer flow was present (case II), wake-like defects were observed in the initial shear-layer profiles because of the inner nozzle lip. Also, inferred from Fig. 6, case II profiles were severely affected by the configuration. This was mainly due to the fact that the exterior geometry of the inner nozzle affected the outer nozzle expansion rate. For example, the main difference between configurations 1 and 3 was the boat-tail angle, which changed the expansion rate of the Mach 1.3 outer flow.

In Fig. 7, the total pressure profiles for different configurations were compared at one streamwise location. The Mach number profiles were deduced using the Rayleigh supersonic pitot formula.[19] While the inner jet profiles for configurations 3–5 were quite similar to the freejet profile in case I, the profiles for configurations 1 and 2 deviated significantly from the others. The major source for the differences in the profiles appeared to be the degree of overexpansion in the outer jet. The ratio between the actual stagnation pressure and the pressure needed to fully expand the outer jet for each configuration was 0.61, 0.61, 0.82, 0.95, and 0.96, respectively. Since the overexpansion of the outer jet changed the static pressure the inner jet would experience at the exit, the inner jet exit pressure was not properly matched in case II.

The similarity of flow profiles for configurations 1 and 2 indicates that the effect of flow straightener on flow development was rather small. Thus, while the flow straightener reduced the freestream turbulence level in the outer jet by about 25%, the shear-layer development appeared to be independent of the initial turbulence fluctuations at least in the present range of fluctuation magnitude. This observation would be applicable as long as the initial level of turbulence magnitude is such that the turbulent kinetic energy in the freestream is much lower than the turbulent energy production in the shear layer. The results also showed that the flow profiles for configurations 4 and 5 were quite similar, suggesting that the actual effect of boat-tail on downstream flow development was rather weak. The flow profiles were most affected when the boat-tail section was placed inside the outer nozzle, because the degree of boat-tail then determined the outer nozzle expansion rate.

Growth Rate Measurements

The shear-layer thickness at any given axial station was defined using the radii that corresponded to 10 and 90% of the freestream total pressure difference. The wake-like defects, which occurred just downstream of the inner nozzle lip with nonzero outer flow, were treated in a similar fashion as that used in Papamoschou and Roshko.[3] However, instead of using the simple difference in radii in estimating the shear-layer thickness, the present measurement considered the cross-sectional area affected by the shear flow. More specifically, the measured shear-layer thickness was defined as the ratio between the cross-sectional area enclosed within the two radii and the perimeter of the reference nozzle.

Such a definition made it possible to compare nonstandard geometry shear layers with an axisymmetric shear layer. Also, it provided a measure of weight for the radial direction in axisymmetric shear layers. For instance, a shear layer spreading radially outward affects a larger cross-sectional area than that spreading inward. This type of imbalance, which does not exist in planar shear layers, can be weighted by the present definition.

The shear-layer thicknesses, measured using both the conventional length-based radial difference approach and the present area-based approach, were plotted vs axial distance

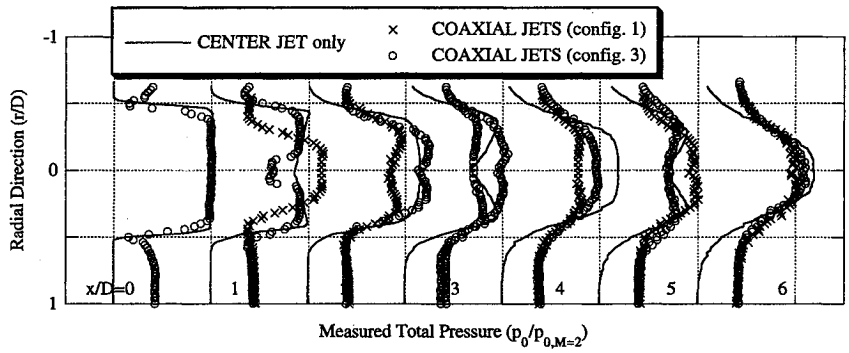

Fig. 6 Axial development of total pressure profiles under different conditions.

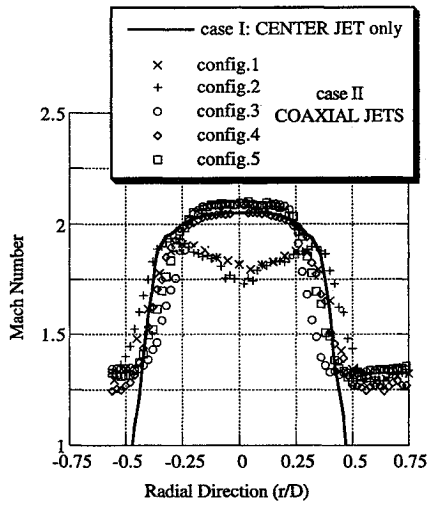

Fig. 7 Comparison of flow profiles at $x/D = 2$.

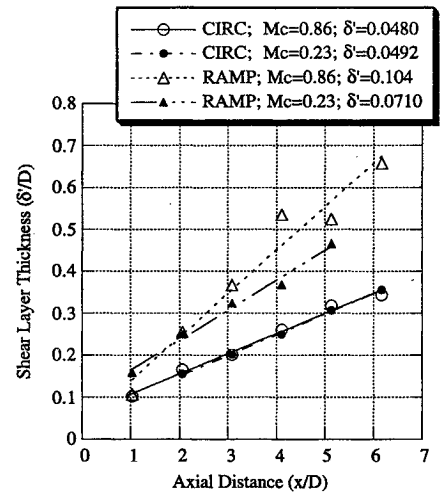

Fig. 9 Average spatial growth of shear-layer thickness as a function of nozzle and flow conditions.

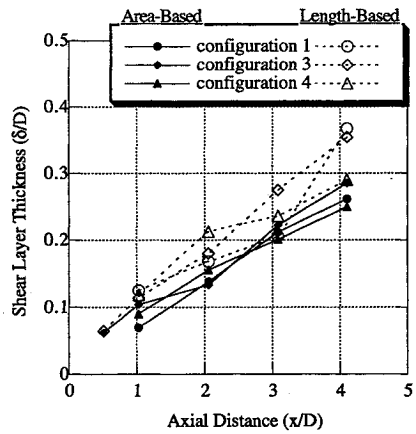

Fig. 8 Shear-layer thickness measurements in the near field of axisymmetric supersonic jets from reference circular nozzles (case II).

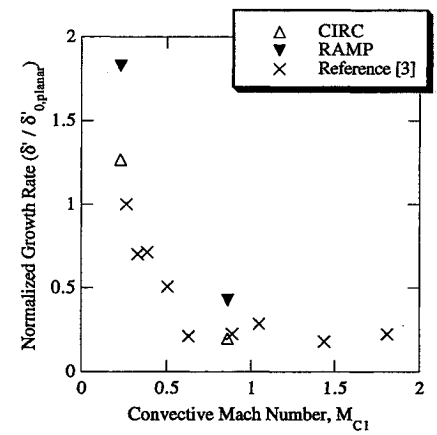

Fig. 10 Normalized shear-layer growth rate using area-based measurement. Planar incompressible growth rate in Ref. 3 was used for normalization.

in Fig. 8 for different configurations. While the length-based measurement of the shear-layer thickness showed an obvious dependence on the nozzle configuration, the data from area-based measurement agreed fairly well. This showed that the present definition of shear-layer thickness was effective in reducing the near-field data scatter from wavy jet-columns caused by exit-pressure mismatch.

Figure 9 shows the comparison of averaged shear-layer thicknesses under various flow and nozzle conditions. The growth rate was obtained from the slope of the least-squared line-fit through the data. It can be clearly seen that the shear-layer growth was expedited with the RAMP nozzle. This observation is further discussed in the following sections.

Effect of Compressibility

For incompressible shear layers, the time rate of growth can be assumed to be proportional to the rate of strain, which in turn is proportional to the freestream velocity difference ΔU. In a frame of reference that moves with the shear-layer velocity U_C, this can be written as

$$\frac{d\delta_0}{dt} = \frac{d\delta_0}{dx}\frac{dx}{dt} = \delta_0' U_C \propto \Delta U$$

where δ_0' is the incompressible shear-layer growth rate. Using

the convective velocity U_C defined previously, Papamoschou and Roshko[3] showed that for pressure profile measurements

$$\delta_0' \approx 0.14(\Delta U/U_C)$$

To assess the effects of compressibility, the actual growth rate for compressible shear layer was compared with δ_0'. Because these effects are well documented in planar shear-layer experiments, the present results from the coaxial setup were compared with planar case. In Fig. 10, the planar incompressible growth rate was used to normalize the present data and the results were compared with the planar compressible shear-layer measurements of Papamoschou and Roshko[3] as a function of the convective Mach number. The results showed that axisymmetric shear layers are similarly affected by the compressibility. Also, while the data for the reference nozzle (CIRC) showed a good agreement with the planar case, the data for RAMP nozzle showed much higher shear-layer growth rate.

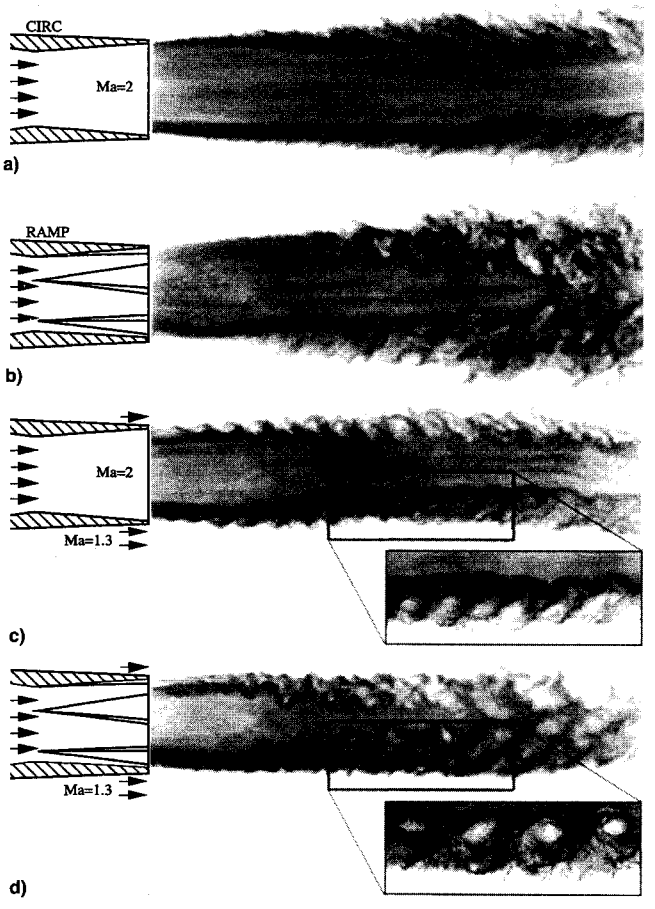

Fig. 11 Planar Mie-scattering images of Mach 2 jets: a) and b) are freejets from CIRC and RAMP nozzles, respectively; c) and d) show the respective jets with a Mach 1.3 coaxial flow. The inserts are high-resolution images of the boxed area taken at other instants.

Effect of Nozzle Geometry: CIRC vs RAMP

Both Figs. 9 and 10 showed that the RAMP nozzle increased the shear-layer growth rate compared to the reference CIRC nozzles. The amount of increase was greater at higher compressibility. At $M_C = 0.86$ (case I), there was about a 110% increase in the shear-layer growth compared to a 44% increase at $M_C = 0.23$.

Figure 11 shows the planar Mie-scattering images of the jets under various nozzle and flow conditions. Inferred from these images, the spatial growth rate of the shear layer was clearly increased with the RAMP nozzle. Figures 11a and 11b show, respectively, the reference jet (CIRC) and the RAMP-expanded jet under the case I condition ($M_C = 0.86$). While the reference shear layer appeared to be unorganized and highly three dimensional, the shear layer for the RAMP-expanded jet was characterized with large-scale lumpy structures with well-defined outlines. The increased spreading rate appeared to be associated with the generation of these structures.

Figures 11c and 11d show the same jets with supersonic outerflow under the case II condition ($M_C = 0.23$). Because of relatively low compressibility, the shear layer for the CIRC jets (Fig. 11c) was also well organized, forming coherent vortices. The shape of coherent vortices for the RAMP jet in Fig. 11d was, however, qualitatively different. Furthermore, there was a clear difference between the structures on the ramp and valley sides, suggesting that the periodic structures were in the transverse plane, i.e., axial vortices. Since large-scale coherent vortices were observed in both CIRC and RAMP jets under the case II condition, the increased shear-layer growth with RAMP jet in this case was then the result of axial vortices.

Figure 12 shows the jet profiles downstream of the RAMP nozzle. The profiles in the near field were characterized by a jagged core that indicated the presence of many oblique shock waves. Also, in the presence of the outer jet (case II), the ramps and valleys modulate the nozzle lip thickness, forming a three-dimensional wake with varying size around the nozzle rim. Then, the interaction of shear layer with the oblique waves and the wake flow could also affect the shear-layer growth.

Chemically Reacting Shear Layer

On the basis of total pressure measurements and visualization images, it was shown that the shear-layer growth rate was enhanced with the RAMP nozzle. Assuming that the mixing rate between the two streams was closely related to the shear-layer growth rate, the reaction rate in chemically reacting shear layers could also be affected.

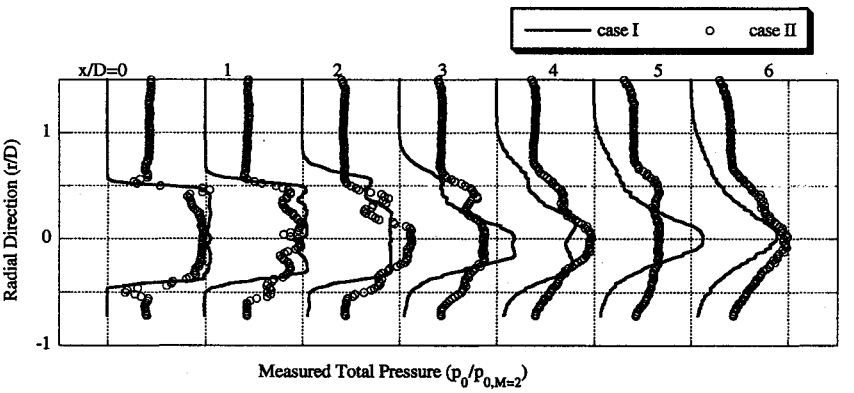

Fig. 12 Total pressure profiles of supersonic jets using the RAMP nozzles.

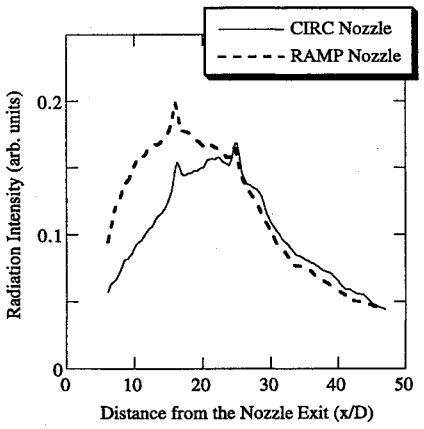

Fig. 13 Bandpass-filtered radiation intensity from Mach 2 afterburning jets.

To create a reacting shear layer, high-temperature combustion products with excess hydrogen were discharged through the inner nozzle. Again, air was used for the outer jet. Afterburning occurred in the shear layer as oxygen in the outer jet mixed with high-temperature hydrogen in the inner jet and reacted. A small but fixed amount of carbon particles was injected and used as an afterburning indicator.

The radiation intensity was measured from the reacting jets using an optical filter with bandpass characteristics of 4.3 ± 0.1 μm. The wavelength corresponds to one of the peaks in a CO_2 absorption spectrum. Although the direct relation between the radiation intensity at this wavelength and the reaction rate was beyond the scope of the present study, it was shown previously that the intensity was related to the reaction of carbon particles in an oxidative environment.[20] In particular, the amount of radiation at this wavelength is related to the temperature and the CO_2 concentration.

When the reacting supersonic jets (case III) discharging from the CIRC and RAMP nozzles were compared, there was a significant difference in average light radiation, particularly from the near-field region of the jets. Figure 13 shows the total radiation intensity, averaged over the test duration and integrated over the transverse dimension, as a function of axial distance from the nozzle. The intensity was much higher with the RAMP nozzle, especially in the near field, indicating an increased amount of reaction. This result implies that the use of the RAMP nozzle affected the rate of mixing as well as the shear-layer spreading.

Summary and Conclusions

Converging–diverging *c/d* supersonic nozzles with mixing enhancement features were tested at three different flow conditions for comparison with circular *c/d* nozzles. Depending on the characteristic features of each nozzle, the nozzles were called NTCH for five notches and RAMP for five ramps built on the expansion side. The jet-spreading performance of the nozzles was compared with that of the reference circular nozzle, called CIRC. All three types of the nozzles were tested at Mach 2, exactly at or very near the design condition. Since the initial total pressure profiles of the jets using the CIRC and the NTCH nozzles were quite similar, only the CIRC and the RAMP nozzles were compared in subsequent tests using coaxial airflow or hot freejet.

For the coaxial jet tests with Mach 1.3 outer flow, five different exterior configurations were used to vary the nozzle exit conditions. The results showed that while various configurations resulted in modified profiles for the shear flow due to outer jet pressure mismatching, the area-based measurement of shear-layer thickness was unaffected by the change. Also, a 25% reduction in the outer stream turbulence level did not significantly affect the inner jet development.

While the shear-layer growth rate associated with the CIRC nozzles showed a reasonable agreement with published planar shear-layer data, significantly higher growth rate was obtained with the RAMP nozzle. The amount of increase was dependent on the convective Mach number M_C with the greater increase obtained at the higher convective Mach number. The increase was 44% at $M_C = 0.23$ (coaxial jet case) and 110% at $M_C = 0.86$ (freejet case).

Planar Mie-scattering flow visualization images were used to compare the qualitative features in the shear layers. The images showed that well-defined, large-scale organized structures, possibly axial vortices, were produced by the RAMP nozzle increasing the shear-layer growth rate. At the lower M_C, the growth-rate enhancement due to the RAMP nozzle was small as the reference shear layer (CIRC) was also characterized by naturally occurring coherent structures. At the higher M_C, the structures of the reference shear layer were unorganized and three dimensional. For this case, the mixing enhancement associated with the RAMP nozzle was even higher.

Finally, the reacting test utilizing high-temperature fuel-rich jets was performed to assess the effect of faster growth of the initial shear layer on the jet afterburning. The result showed that the total combustion rate was clearly modified with the RAMP nozzle. For the particular condition tested, the effect of the RAMP nozzle was to increase the combustion rate in the near field of the jet. This suggests that the RAMP nozzle can be used to improve the mixing process in supersonic reacting jets.

Acknowledgments

This research was sponsored by Gabriel D. Roy of the Office of Naval Research. Also, during the period in which the investigation was performed, the first author received an ONR postdoctoral fellowship administered by the American Society for Engineering Education.

References

[1]Bogdanoff, D. W., "Compressibility Effects in Turbulent Shear Layers," *AIAA Journal*, Vol. 21, No. 6, 1983, pp. 926, 927.

[2]Chinzei, N., Masuya, G., Komuro, T., Murakami, A., and Kudou, K., "Spreading of Two-Stream Supersonic Turbulent Mixing Layers," *Physics of Fluids*, Vol. 29, No. 5, 1986, pp. 1345–1347.

[3]Papamoschou, D., and Roshko, A., "The Compressible Turbulent Shear Layer: An Experimental Study," *Journal of Fluid Mechanics*, Vol. 197, 1988, pp. 453–477.

[4]Gutmark, E., Schadow, K. C., and Wilson, K. J., "Effect of Convective Mach Number on Mixing of Coaxial Circular and Rectangular Jets," *Physics of Fluids A*, Vol. 3, No. 1, 1991, pp. 29–36.

[5]Coles, D., "Dryden Lecture: The Uses of Coherent Structures," AIAA Paper 85-0506, Jan. 1985.

[6]Dimotakis, P. E., "Turbulent Free Shear Layer Mixing," AIAA Paper 89-0262, Jan. 1989.

[7]Ho, C. M., and Gutmark, E., "Vortex Induction and Mass Entrainment in a Small-Aspect-Ratio Elliptic Jet," *Journal of Fluid Mechanics*, Vol. 179, 1987, pp. 383–405.

[8]Schadow, K. C., Gutmark, E., Parr, D. M., and Wilson, K. J., "Selective Control of Flow Coherence in Triangular Jets," *Experiments in Fluids*, Vol. 6, 1988, pp. 129–135.

[9]Bradbury, L. J. S., and Khadem, A. H., "The Distortion of a Jet by Tabs," *Journal of Fluid Mechanics*, Vol. 70, 1975, pp. 801–813.

[10]Longmire, E. K., Eaton, J. K., and Elkins, C. J., "Control of Jet Structure by Crown-Shaped Nozzle Attachments," AIAA Paper 91-0316, Jan. 1991.

[11]Samimy, M., Reeder, M., and Zaman, K., "Supersonic Jet Mixing Enhancement by Vortex Generations," AIAA Paper 91-2263, June 1991.

[12]Northam, G. B., Capriotti, D. P., Byington, C. S., and Greenberg, I., "Mach 2 and Mach 3 Mixing and Combustion in Scramjets," AIAA Paper 91-2394, June 1991.

[13]Marble, F. E., Hendricks, G. J., and Zukoski, E. E., "Progress Toward Shock Enhancement of Supersonic Combustion Processes,"

AIAA Paper 87-1880, June 1987.
[14]Waitz, I. A., Marrble, F. E., and Zukoski, E. E., "An Investigation of a Contoured Wall Injector for Hypervelocity Mixing Augmentation," AIAA Paper 91-2265, June 1991.
[15]Northam, G. B., Greenberg, I., and Byington, C. S., "Evaluation of Parallel Injector Configurations for Supersonic Combustion," AIAA Paper 89-2525, July 1989.
[16]Davis, D. O., and Hingst, W. R., "Progress Toward Synergistic Hypermixing Nozzles," AIAA Paper 91-2264, June 1991.
[17]Clemens, N. T., and Mungal, M. G., "A Planar Mie Scattering Technique for Visualizing Supersonic Mixing Flows," *Experiments in Fluids*, Vol. 11, 1991, pp. 175–185.
[18]Messersmith, N. L., Dutton, J. C., and Krier, H., "Experimental Investigation of Large Scale Structures in Compressible Mixing Layers," AIAA Paper 91-0244, Jan. 1991.
[19]Liepmann, H. W., and Roshko, A., *Elements of Gasdynamics*, Wiley, New York, 1957, pp. 148, 149.
[20]Kraeutle, K., Wilson, K., Lee, M., Gutmark, E., and Schadow, K., "The Effects of Particles on Afterburning and Thermal Images of Plumes," AIAA Paper 91-0182, Jan. 1991.